Proceedings of ERAD (2002): 428–432 © Copernicus GmbH 2002

ERAD 2002

UHF-radar investigations of low-tropospheric mesoscale dynamical processes: cases of mistral

V. Guénard[1], **J. L. Caccia**[1], **B. Campistron**[2], **and P. Drobinski**[3]

[1]Laboratoire de Sondages Electromagnétiques de l'Environnement Terrestre , Université de Toulon et du Var, Toulon, France
[2]Laboratoire d'Aérologie, Université Paul Sabatier, Toulouse, France
[3]Service d'Aéronomie, Université Pierre et Marie Curie, Paris, France

Abstract. UHF-radar wind profilers provide the temporal evolution of the wind velocity and reflectivity vertical profiles from 150/300 m to 2000/4000 m of altitude, with a vertical resolution of 150 m and a temporal resolution of 5 min., by measuring the received clear-air doppler shift of the transmitted frequency (here around 1 GHz) due to the air mass turbulent motions. Those experimental parameters show the pertinence of such instruments in low- tropospheric mesoscale dynamical process studies, mainly when the scientific objectives require the knowledge of the evolution of the air flow vertical structure.

The observations presented here were made during the MAP (fall 1999) and ESCOMPTE (summer 2001) campaigns, for which UHF radars were installed in south-eastern France, and concern experimental studies of Rhne-valley wind regimes, called Mistral, when the air masses approach the mediterranean coast. Although the importance of this wind regime for the meteorological conditions of such areas is well established, it has been only poorly scientifically studied. One important reason was the absence of instruments able to monitor its vertical structure. As we show here UHF radars have this ability.

The results consist of time-height diagrams of horizontal wind, vertical velocity and UHF reflectivity profiles interpreted in a coastal meteorology context. More accurately, the divergence and the subsidence of the flow after exiting the Rhne valley, the effects of the synoptic situation evolution, the main differences between fall and summer cases and the induced boundary layer variations are investigated. In addition to this experimental approach some comparisons with mesoscale numerical model, here mesoNH, are also presented.

Correspondence to: V. Guénard (guenard@lseet.univ-tln.fr)

1 Introduction

UHF-radar wind profilers have already proved their capabilities to investigate the dynamics of the atmospheric boundary layer via the retrieval of the three components of the wind (e.g. Atlas, 1990). Owing to their vertical and time resolutions, they are suited to study mesoscale aspects of a low-tropospheric wind regime, as the Mistral studied here.

The Mistral is a northerly wind blowing in South of France. Various kinds of causes may trigger the Mistral, however, the most frequent one is the passage of a cut-off low above the Alps from the north west, associated with a cold front. This meteorological situation often triggers a surface low in the wake of the Alps which in turn triggers the onset of a northerly wind channeled by the Rhône valley and enhanced by an anticyclonic ridge on a Spain-Massif Central axis; this process is called the Genoa Gulf cyclogenesis. Figure 1 depicts this kind of synoptic forcing. At the exit of the Rhône valley and approaching the Mediterranean coast, the air masses go down and accelerate, due to the rugosity decrease and then rotate southeastward. Due to its mesoscale features and to the needs of numerous experimental means to investigate it in details, none or few scientific studies have concerned the horizontal, vertical and time evolution of the Mistral after the exit of the Rhône valley. For instance, Pettré (1982) studied the Mistral in the Rhône valley and attempted to explain its acceleration along the valley by means of the 2D hydraulics theory.

The field experiments MAP (Mesoscale Alpine Program, autumn 1999, Bougeault et al., 2001) and ESCOMPTE (Expérience sur Site pour COntraindre les Modèles de Pollution atmosphérique et de Transport d'Emissions, June–July 2001, http://medias.obs-mip.fr/escompte) took place over the region concerned by the Mistral and gave the opportunity to better investigate this mesoscale meteorological phenomenon. The MAP general objective is to improve the understanding of mesoscale processes around and above the Alps, and the split winds, as the Mistral, is one of the specific scientific objectives. ESCOMPTE concerned pollution

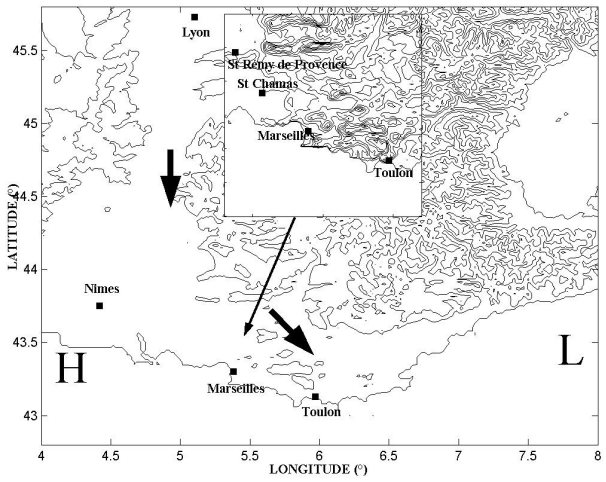

Fig. 1. Region of interest and location of UHF profilers during MAP and ESCOMPTE. Black thick arrow's indicate the Mistral most frequent direction. H is the ridge of the eastern Atlantic anticyclone. L is the Genoa Gulf though.

emissions and transport in the area of Aix-Marseilles-Berre pond (south of France). Mistral studies are not a scientific objective of the campaign since it decreases the pollution in the area, however, several cases of Mistral occured during the period. Owing to the high spatial density of the measurement network, the "summer" Mistral might be well characterized as well as its interaction with land-sea breezes.

For each campaign, data from two UHF radars are used and analysed here: one installed at St-Chamas (north-west from Marseilles) and one at Toulon (south-east from Marseilles), for MAP, and one at St-Chamas and one at Marseilles, for ESCOMPTE (see Fig. 1).

2 UHF-radar data

2.1 Wind retrieval

Before profiler data can be used, they must be subjected to quality control to remove contamination from precipitation, birds, radio frequency interference and other sources. Data that do not support the quality control test are plotted in white on the surface color diagrams displayed in Sect. 3. UHF Degréane wind profilers, used here, work with a mean power of 40° W, at a frequency of 1.238 GHz. Returned echoes are due to the air refractive index fluctuations advected by the wind. The three wind components are obtained from the frequency Doppler shift obtained along five beam directions: one vertical and two oblique pairs, symmetrical with respect to the vertical and in two perpendicular vertical planes. The errors on the horizontal winds is and the vertical velocity are typically, and respectively, 1–2 m.s^{-1} and 0.25–0.5 m.s^{-1}. Data measured here are obtained every 15 min. from a height of 100–300 up to 2500–4000 m Above Ground Level (AGL) with a 75–150 m vertical resolution (Caccia et al., 2001). Such experimental parameters show that UHF profilers are well suited for mesoscale studies of low troposhere phenomena.

2.2 Thermal advection retrieval

Thermal advection is quite difficult to measure or to extract directly because of space and time differenciating scale. The relatively high space-time resolution of wind profilers is relevant to assess the trend of the thermal advection. The VHF-profiler method to obtain it (Crochet et al., 1990) has never been processed to UHF investigations of the low-level jets as the Mistral. On the assumption of an adiabatic atmosphere, the thermal advection At is given by the expression (1):

$$At = \frac{f}{R_w}\boldsymbol{k} \cdot \left(\boldsymbol{V}_g \times \frac{\partial \boldsymbol{V}_g}{\partial \log P}\right) = -\boldsymbol{V}_g \cdot \boldsymbol{\nabla}_P T \qquad (1)$$

where $\boldsymbol{V}_g$ is the geostrophic wind (under our assumption $\boldsymbol{V}_g$ is taken as the horizontal wind measured by the radar), P the pressure , $f = 10^{-4}$ s^{-1} the Coriolis parameter, R_w the wet air constant (supposed to be equal to the dry air constant R = 287 J·kg^{-1}·K^{-1} since the Mistral associated is a dry wind) and $\boldsymbol{k}$ the vertical unity vector.

2.3 C_N^2 profiles and ABL height

UHF wind profilers are sensitive to clear air refractive index fluctuations related to temperature and humidity fluctuations in the resolution volume. Turbulence at scale of the radar half-wavelength (here 12 cm) is the main factor leading to fluctuations of the air refractive index, and is characterized by its structure constant C_N^2. Ottersten (1969) gave the relation between C_N^2, the radar reflectity η and the radar wavelength λ.

$$\eta = 0.38\lambda^{-1/3}C_N^2, \qquad (2)$$

whereas the expression of the reflectivity as a function of radar parameters is given by Van Zandt et al. (1978):

$$\eta = 9\pi k_0 B(ET_C + T_{rx})\left(\frac{R}{\Delta R}\right)^2 \frac{SNR}{P_t F_r A_e E^2} \qquad (3)$$

where c is the light speed, k_0 the Boltzman constant, B the integrator filter bandwith, E the radar antenna efficiency, T_c the cosmic noise temperature, T_{rx} the receiver noise temperature, R the radial distance, ΔR the radial resolution of the radar, SNR the signal to noise ratio, P_t the crest pulse power, F_r the pulse frequency, A_e the effective area of the antenna. Therefore, C_N^2 profiles can be obtained from the radar parameters and by using the expressions (2) and (3).

The height, Z_i, of the ABL (defined as the atmospheric layer directly influenced by the ground) is detectable, either from the first location of the strong potential temperature gradient (Sullivan et al., 1998), either from the location of the C_N^2-profile maximum value (Jacoby-koaly, 2000). The ABL height is of primal interest for hydraulics theory and is a key parameter to understand the Mistral (Pettré, 1982).

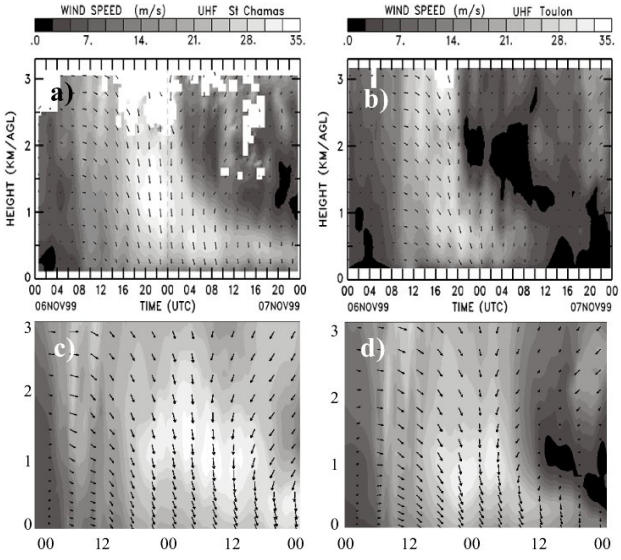

Fig. 2. Horizontal wind speed (gray filled) and direction (arrows) observed by UHF wind profilers of **(a)** St-Chamas, **(b)** Toulon, simulated by MESO-NH at **(c)** St-Chamas, **(d)** Toulon.

3 Results and discussion

3.1 An autumn Mistral case (MAP 6–8 November 1999)

During the MAP IOP 15, a strong Mistral event was observed. The onset of the Mistral occured the 6 November 1999 and was characterized by the features described in Sect. 1. The time evolution of the horizontal wind profiles (Figs. 2a, 2b) observed by the radars of St Chamas and Toulon shows that the onset of the Mistral is simultaneous in both sites, however, the wind is stronger at St-Chamas (with maximum speed of 35-40 m.s^{-1} at 1200 m AGL) than at Toulon (maximum speed of 30 m.s^{-1} at 700 m AGL). Furthermore, the wind is clearly northerly at St-Chamas, whereas the wind blows southeastward at Toulon. Another feature of this Mistral case is the shift of the wind vertical structure occuring at 04:00 UTC 7 November 1999. Before this time, the wind blows on the total depth investigated by the UHF wind profiler and, after this time, a "shallow Mistral" confined below 1500 m AGL is observed. This behavior is rather well reproduced by simulations from the non-hydrostatic mesoscale numerical model, meso-NH (Lafore et al., 1998), carried out at the vertical of the two radars (Fig. 2c, 2d), despite an overestimation of the duration of the Mistral event (Figs. 2c, 2d). These discrepancies may be explained by a sharp intense horizontal wind gradient (~ 3 ms$^{-1}\cdot$ km^{-1}) moving westward splitting a sheltered zone at the east side of Toulon from a zone of intense wind (figure not shown) and having a typical horizontal scale smaller than the model gird scale (here 27 km).

The time evolution of the vertical velocity (Figs. 3a, 3b) is 60 min. averaged in order to filter the mountain waves occuring in Mistral situations (Pettré, 1982) and illustrates

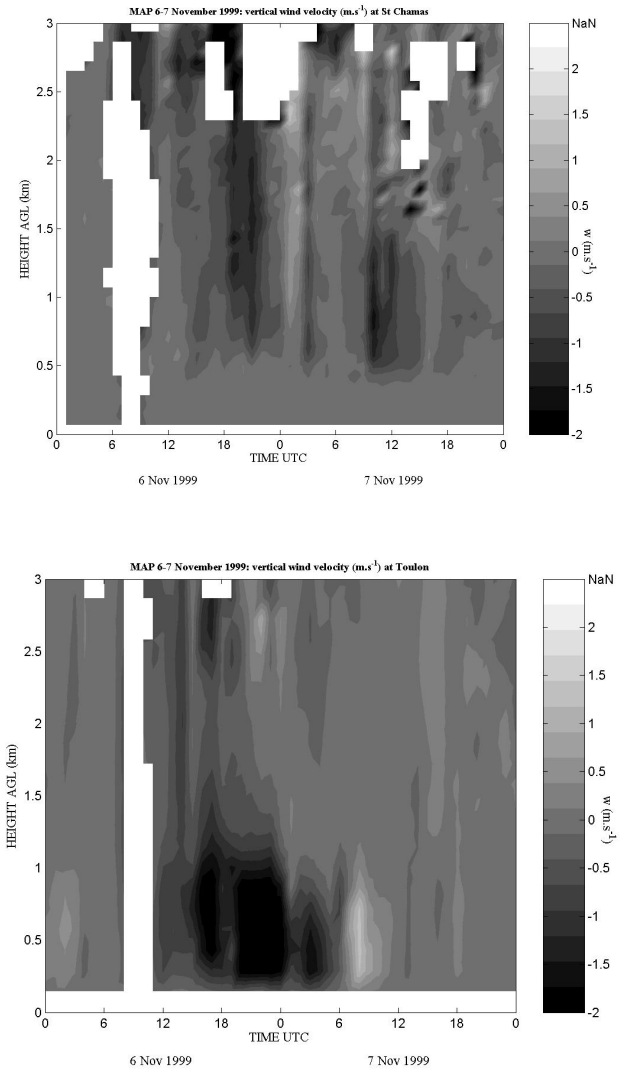

Fig. 3. MAP IOP 15 Mistral event (6–7 November 1999) vertical wind velocities (m.s-1) observed at **(a)** St-Chamas and **(b)** Toulon.

the downward motions of air masses due to several possible factors: cold and denser air reaching the sea, anticyclonic subsidence, seaward decrease of the mean rugosity, strong local forcing by the near topography (Mount Faron 700 m at Toulon) inducing downslope winds (Smith, 1985).

The radar-derived time evolution of thermal advection is plotted (Figs. 4a, 4b) for St-Chamas and Toulon. Notice the strong cold advection of magnitude $\sim -3^\circ$ C$\cdot$ h^{-1} associated with the Mistral jet in both sites. This feature is not so surprising considering Mistral brings polar air masses. However, taking into account the temperature trend extracted from radiosoundings (not shown), thermal advection seems to be overestimated of 1° C $\cdot$h^{-1}. Various causes may explain this discrepancy but the major one is the assumption on the equality of the radar-derived winds with the geostrophic winds. Thermal advection values are likely false below 1500 m where orography plays a significant role in wind flow in-

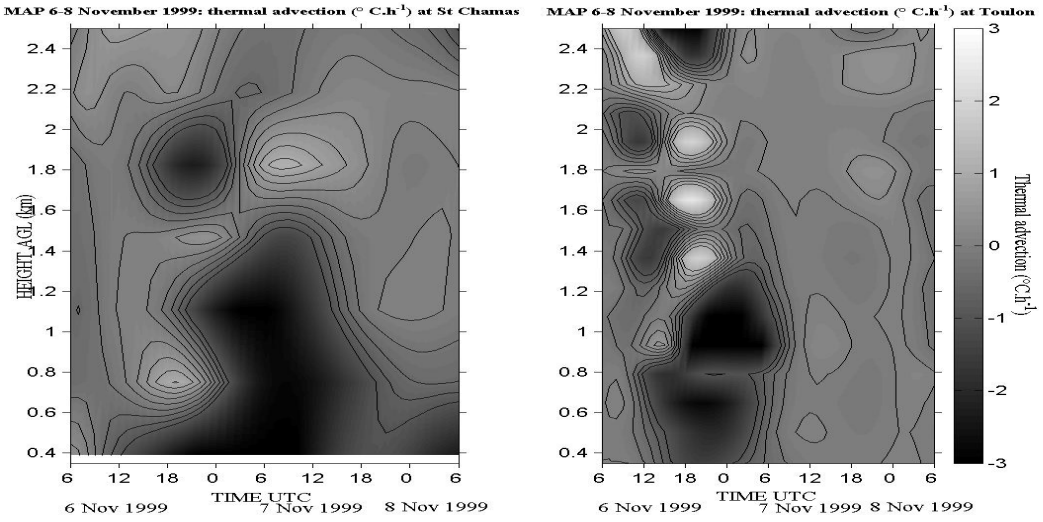

Fig. 4. MAP 6–8 November 1999, thermal advection ($^\circ$ C·h^{-1}) computed from expression (1) at **(a)** St-Chamas and **(b)** Toulon.

ducing not negligible ageostrophic wind components. Thus, this assumption induces more wind shears in low levels than real geostrophic shears, increasing the magnitude of thermal advection. On the other hand, the assumption of an adiabatic atmosphere is valid since it is well known that Mistral winds are associated with dry air. Notice that the sea breeze phenomenon is avoided in this autumn case, but wind direction shift may occur at the sea-land transition.

Nevertherless, the technique presented here is easy to set up and allows a retrieval of thermodynamical features of regional winds at a better resolution than radiosounding data, launched every 6 h. This technique may be improved by integrating wind corrections to reach a best approximation of the geostrophic wind in low levels.

3.2 A summer Mistral case: 16–19 June 2001

During ESCOMPTE, a Mistral event occured the 16 June 2001, 12:00 UTC. The winds have blown southeastward the 16–17 June, increasing in strength the 18 June morning, with a maximum speed of 25 m·s^{-1} at 06:00 UTC and at 1km AGL (Fig. 5a). Then, the winds have taken a southward direction. The erosion phase of this Mistral event is resembling the one of the autumn Mistral case described in Sect. 3.1: first above 1500 m at noon of 18 June and then, in lower levels during the second part of the day. Considering that the structure of the wind is the same as in the autumn Mistral case, the time evolution of thermal advection, which depends of shears, presents about the same feature than that displayed in Fig. 4 and is not plotted here.

On the other hand, the ABL height, Z_i, retrieved from the maximum C_N^2 criterion is displayed in Fig. 5b. Black circles are the maxima of C_N^2. The black squares represents the ABL height extracted from the radiosounding of Nimes launched every 12 h (for site location, see Fig. 1) and the dashed line is the ABL height from the radiosounding of St-Remy de Provence launched every 3 h the 17 June 2001. In both cases the method of Sullivan et al. (1998) is used to retrieve Z_i (see Sect. 2.3.).

The time evolution of the maxima of C_N^2 (Fig. 5b) shows a diurnal variation in agreement with the basic knowledge of ABL height variations: Z_i increases during the morning with convective motions due to the ground heating while Z_i decreases, during the night, resulting from ground cooling. When Mistral blows, Z_i is less well marked than in calm situations. Indeed, 19 June 2001, the CN2 maxima are much more visible and less dispersed after the wind has stopped than the days before. Z_i values extracted from radiosounding and those from UHF profilers are compatible regarding the site location differances. Indeed, notice the large disagreement between Z_i values from both radiosoundings on the 17 June 2001, 12:00 UTC. This illustrates the strong dependence of Z_i with the site location, so care must be taken with wind profiler/radiosounding data comparisons.

4 Conclusions and future works

UHF wind profiler is a useful and efficient tool to investigate the atmospheric boundary layer. It is able to measure with high space and time resolution the three wind components between 200 and 3000 m. Thus, it is suited for the validation of the non-hydrostatic mesoscale numerical models. Its high resolution and accuracy allow studies on mesoscale atmospheric processes such as the Mistral blowing in South of France. Other meteorological parameters have been derived from UHF profilers and are the following.

Time evolution of thermal advection exhibits a good agreement with the basical knowledge of the Mistral: a well marked cold advection ($\sim -3^\circ$ C·h^{-1}), associated with the flow, has been found. Now, the technique to retrieve thermal advection may be improved by introducing corrections

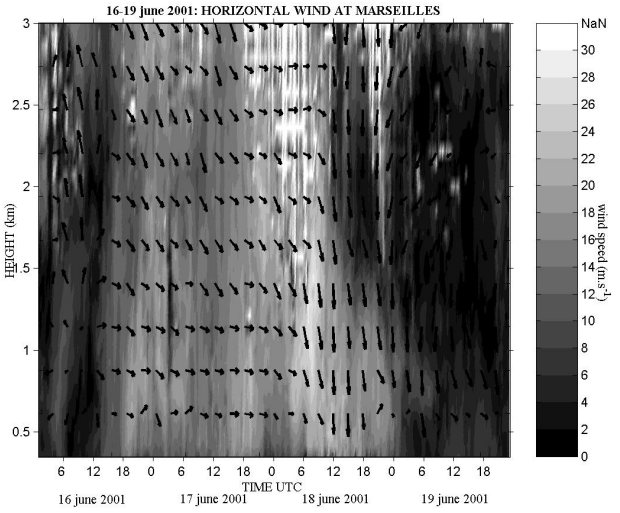

(a)

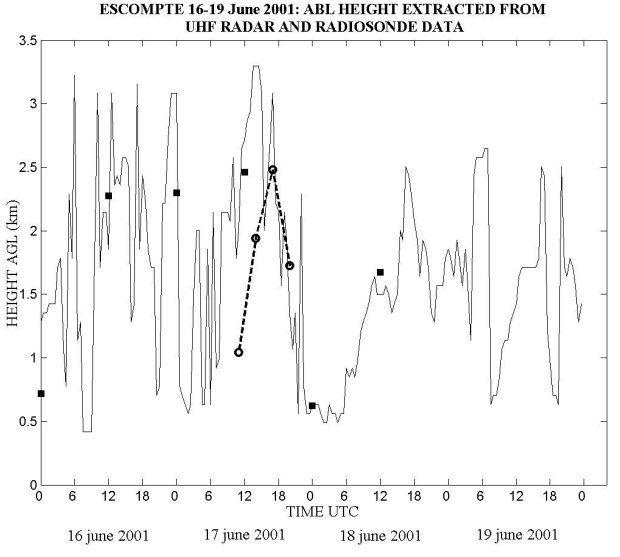

(b)

Fig. 5. 16–19 June 2001 Mistral event at Marseilles. **(a)** horizontal wind speed (gray filled) and direction (arrows) observed by the UHF wind profiler. **(b)** ABL height at Marseilles extracted from the UHF CN2 maximum criterion (solid line) and from radiosoundings of Nimes (black squares) and St Remy de Provence (dashed line).

to better reach geostrophic wind shears in low levels. Moreover some questions remains about Mistral thermal advections: is there any meteorological situation leading to "warm Mistral"? In all the cases, the calculation method presented here is the first step toward an analysis of thermodynamical aspects of regional wind by only means of UHF profilers.

The use of C_N^2 profiles to assess the ABL height provides good results in well developped ABL (here in summer and in absence of wind). If the Mistral blows, the retrieval is complicated by its interaction with thermal convection. The algorithm used in this study should be tested its efficiency on autumn and winter Mistral situations and will form the subject of future works. They will consist on data comparisons between wind profiler and colocated radiosounding station (data not available yet).and airborne doppler lidar data for a 3D approach (Drobinski et al., 2002).

References

Atlas, D., Radar in meteorology, AMS, 1990.

Bougeault, P., Binder, P., Buzzi, A., Dirks, R., Houze, R., Kuettner, J., Smith, R.B., Steinacker, R., Volkert, H., The MAP Special Observing Period, Bull. Amer. Meteor. Soc., 82, 433–462, 2001.

Caccia, J.L., at al., The french st-radar network during map: observational and scientific aspects, Meteor. Z., 10, 6, 469–478, 2001.

Crochet, M., Bazile, E., Rougier, G., Comparison of thermal advection measurements by clear-air radar and radiosondes techniques, Radio Sci., 25, 4, 907–915, 1990.

Drobinski, P., and Coauthors, Characterization of the 28 June 2001 Mistral event during the ESCOMPTE field experiment, in Proc. of 10th AMS conf. on mountain meteorology, 17–21 June, Park City, USA, 2002.

Jacoby-koaly, S., Application d'un radar profileur de vent UHF à l'étude de la couche limite atmosphérique, Ph.D. thesis, Université P. Sabatier, Toulouse, France, 176 pp., 2000.

Lafore, J.P., Stein, J., Asencio, N., Bougeault, P., Ducrocq, V., Duron, J., Fischer, C., Hreil, P., Mascart, P., Masson, V., Pinty, J.P., Redelsperger, J.L., Richard, E., Vilà-Guerau de Arellano, J., The Meso-NH atmospheric simulation system. Part I: adiabatic formulation and control simulations, Ann. Geophys., 16, 90–109, 1998.

Ottersten, H., Atmospheric structure and radar backscattering in clear air atmosphere, Radio Sci., 4, 1179–1193, 1969.

Pettré, P., On the problem of violent valley wind, J. Atmos. Sci. ,39,3, 542–554, 1982.

Smith, R.B, On severe downslope winds, J. Atmos. Sci, 42, 2597–2603, 1985.

Sullivan, P.P., Moeng, C.H., Stevens, B., Lenschow, D.H., Mayor, S.D., Structure of the entrainment zone capping the convective atmospheric boundary layer, J. Atmos. Sci., 55, 19, 3042–3064, 1998.

Van Zandt, T.E., Green, J.L., Gage, K.S., Clark, W.L., Vertical profiles of refractivity turbulence struture constant: comparison of observations by the sunset radar with a new theoretical model, Radio Sci., 13, 819–829, 1978.